A light scattering grid for irregular lunar dust grains: A resource for surface and orbital investigations

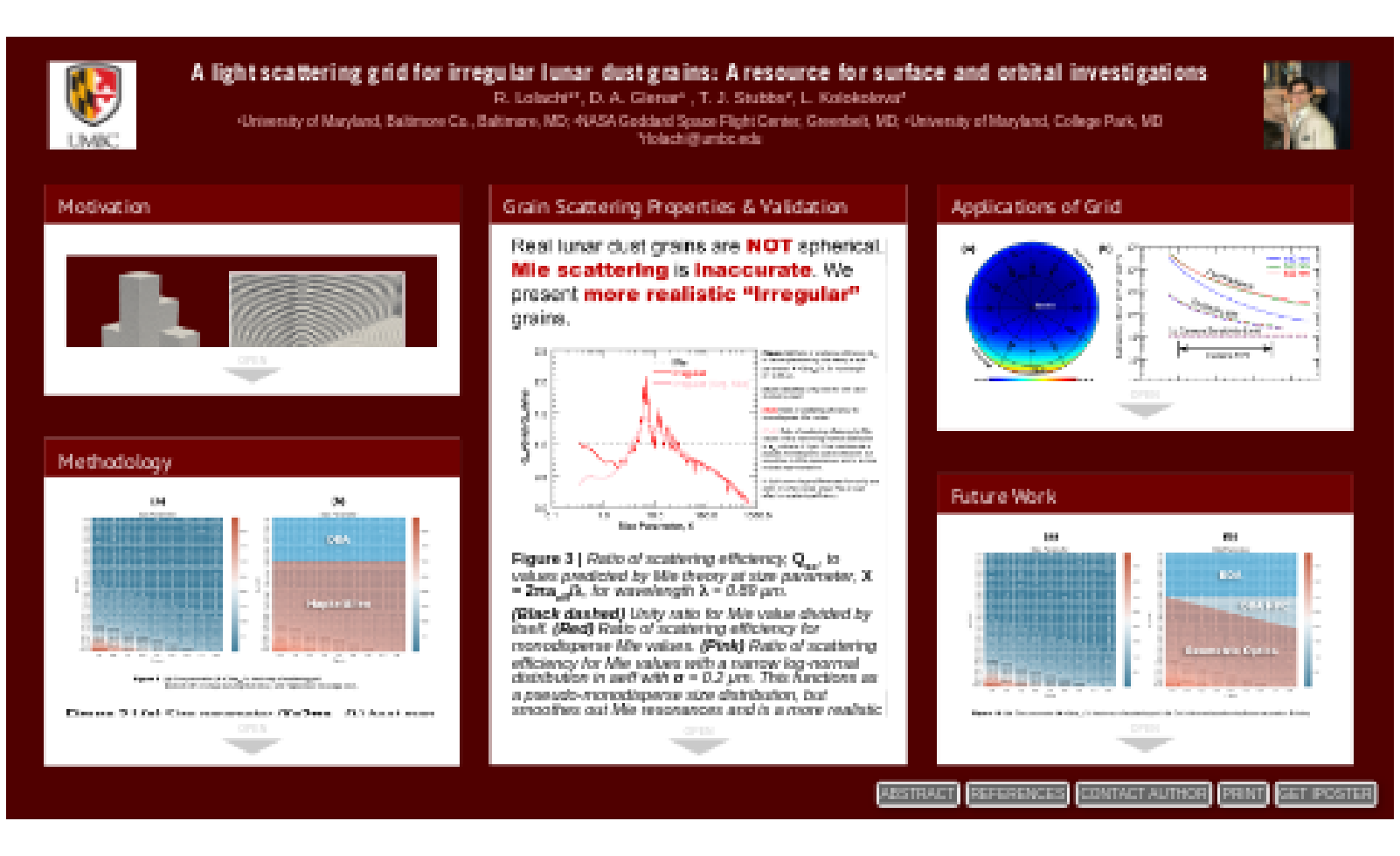

R. Lolachi[1]*, D. A. Glenar[1], T. J. Stubbs[2], L. Kolokolova[3]

[1]University of Maryland, Baltimore Co., Baltimore, MD; [2]NASA Goddard Space Flight Center, Greenbelt, MD; [3]University of Maryland, College Park, MD
*rlolachi@umbc.edu

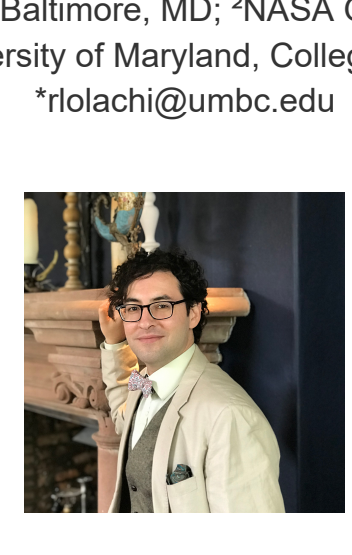

PRESENTED AT:

AGU FALL MEETING
Online Everywhere | 1–17 December 2020

MOTIVATION

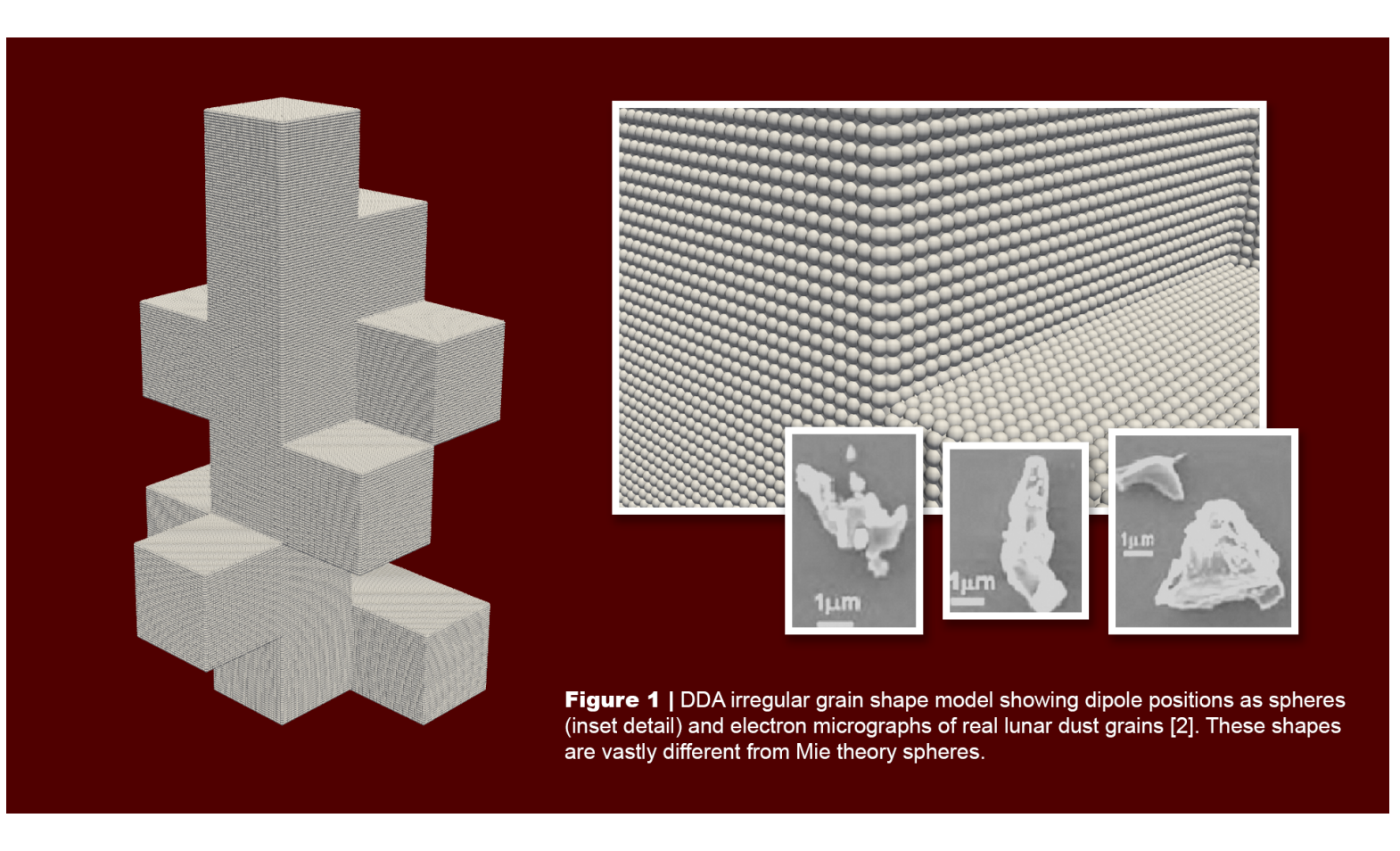

Figure 1 | *DDA irregular grain shape model showing dipole positions as spheres (inset detail) and electron micrographs of real lunar dust grains [2].* ***These shapes are vastly different from Mie theory spheres.***

Observations and simulations of sunlight scattering by dust are critical as they provide lunar science (e.g., giving dust composition, shape, and abundance, revealing history of surface evolution) and also inform future human exploration (e.g., dust environment abundance measurements for risk mitigation). Both projects require more realistic dust grain scattering properties than offered by Mie theory (real dust grains are not spherical). Hence, we present a scattering properties grid for realistic irregular-shaped lunar dust grains.

METHODOLOGY

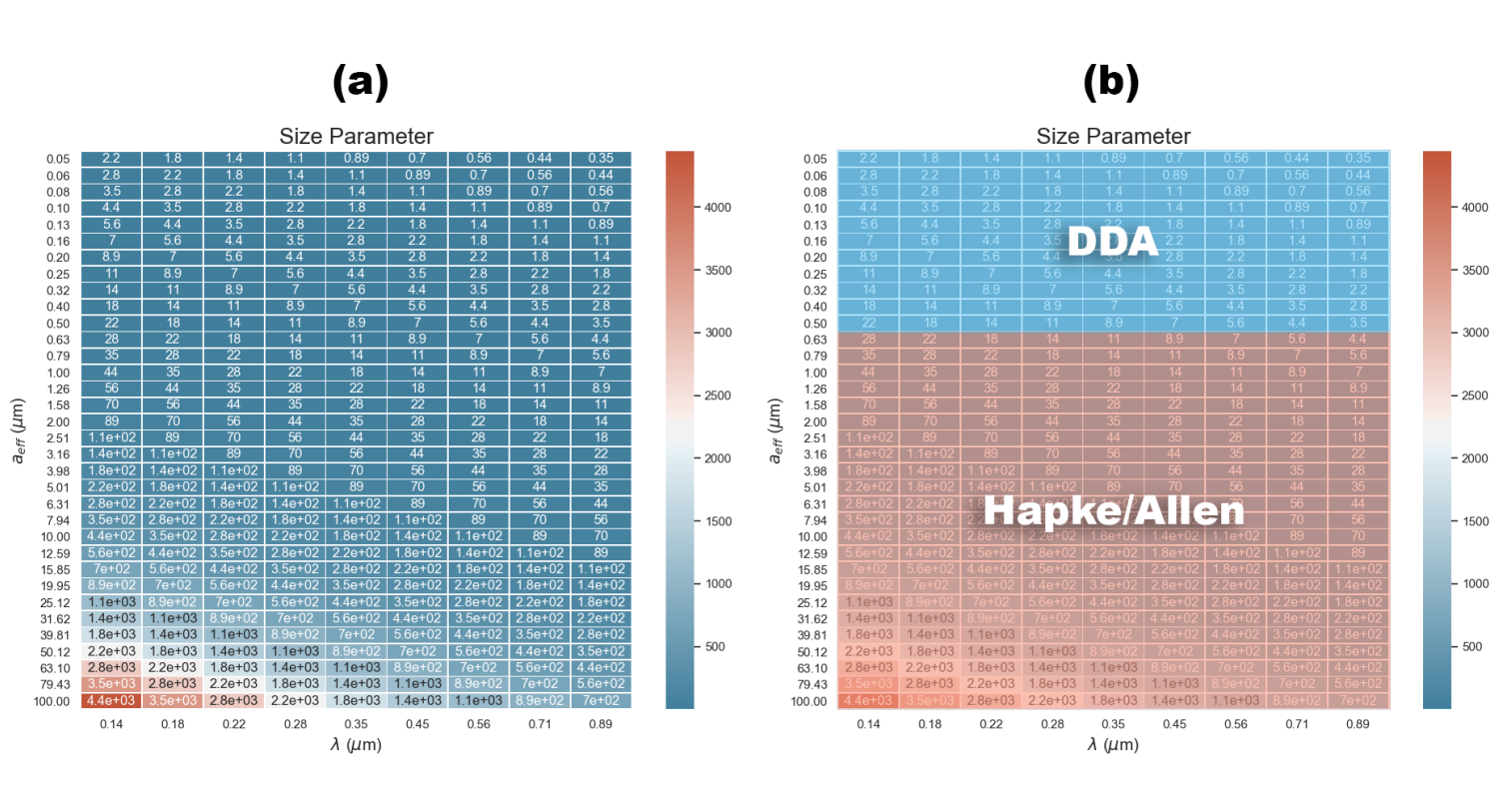

Figure 2 | ***(a)*** *Size parameter (**X=2πa$_{eff}$/λ**) heat map of scattering grid.*

(b) *Grid with overlays showing DDA (blue) and Hapke/Allen coverage (red).*

X: Effective Radius ***Y:*** *Wavelength*

- Scattering property (scattering coefficients, phase functions, and polarization) interpolation grids of lunar "Irregular" grains were computed using the Discrete Dipole Approximation (DDA) method [2] for smaller grains (effective radius $0.05 \le a_{eff} \le 0.5$ µm).
- Larger grains (effective radius $0.5 < a_{eff} \le 100$ µm) are computed using the Hapke equivalent-slab method with Allen diffraction.
- Wavelength coverage of 0.14–0.89 µm with grain refractive indices are "Average Moon" values of Shkuratov et al. [3].

GRAIN SCATTERING PROPERTIES & VALIDATION

Real lunar dust grains are NOT spherical. Mie scattering is inaccurate. We present more realistic "Irregular" grains.

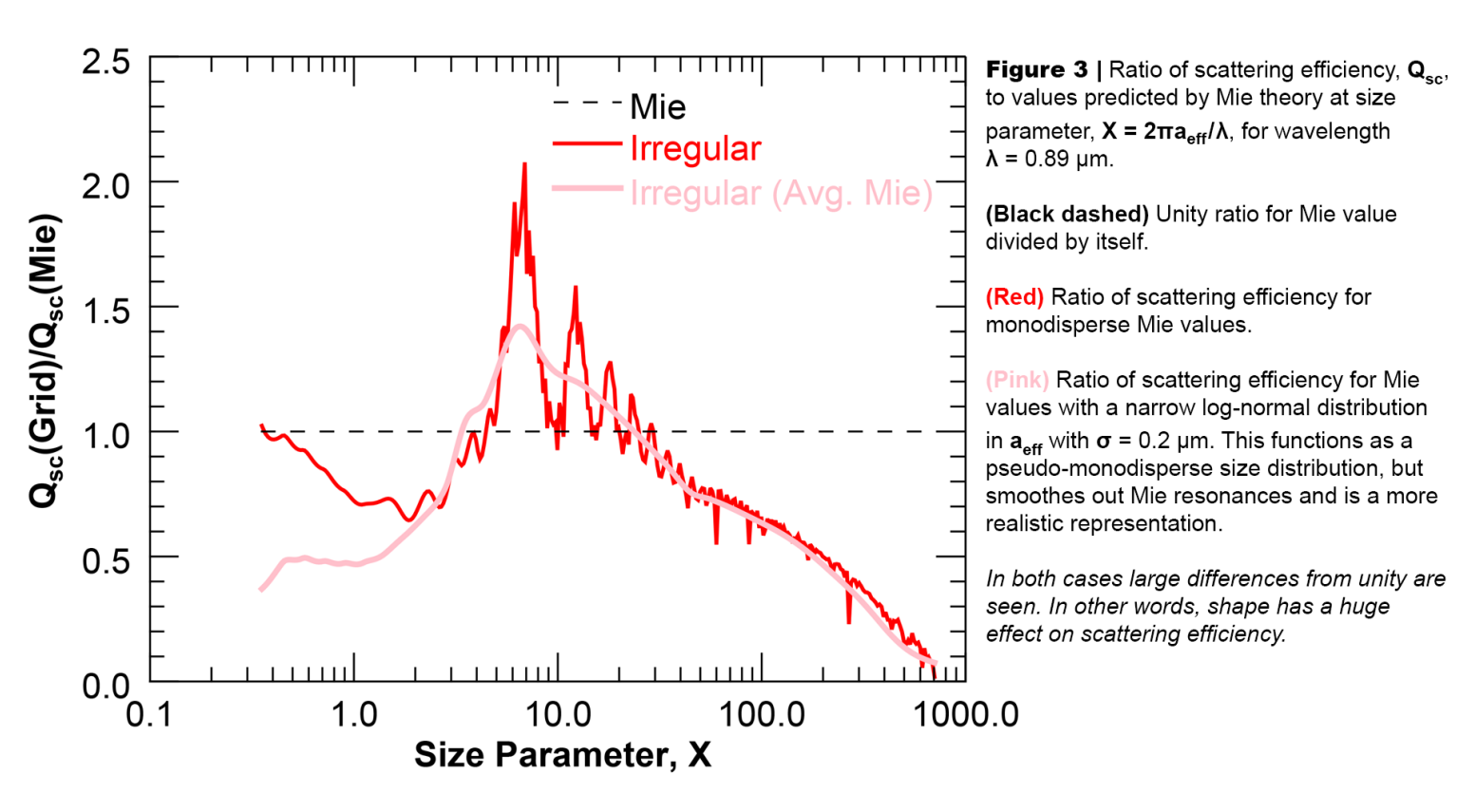

Figure 3 | *Ratio of scattering efficiency,* **Q_{sc}**, *to values predicted by Mie theory at size parameter,* **X = 2πa$_{eff}$/λ**, *for wavelength* **λ** *= 0.89 µm.*

(Black dashed) *Unity ratio for Mie value divided by itself.* ***(Red)*** *Ratio of scattering efficiency for monodisperse Mie values.* ***(Pink)*** *Ratio of scattering efficiency for Mie values with a narrow log-normal distribution in aeff with* **σ** *= 0.2 µm. This functions as a pseudo-monodisperse size distribution, but smoothes out Mie resonances and is a more realistic representation.* ***In both cases large differences from unity are seen. In other words, shape has a huge effect on scattering efficiency.***

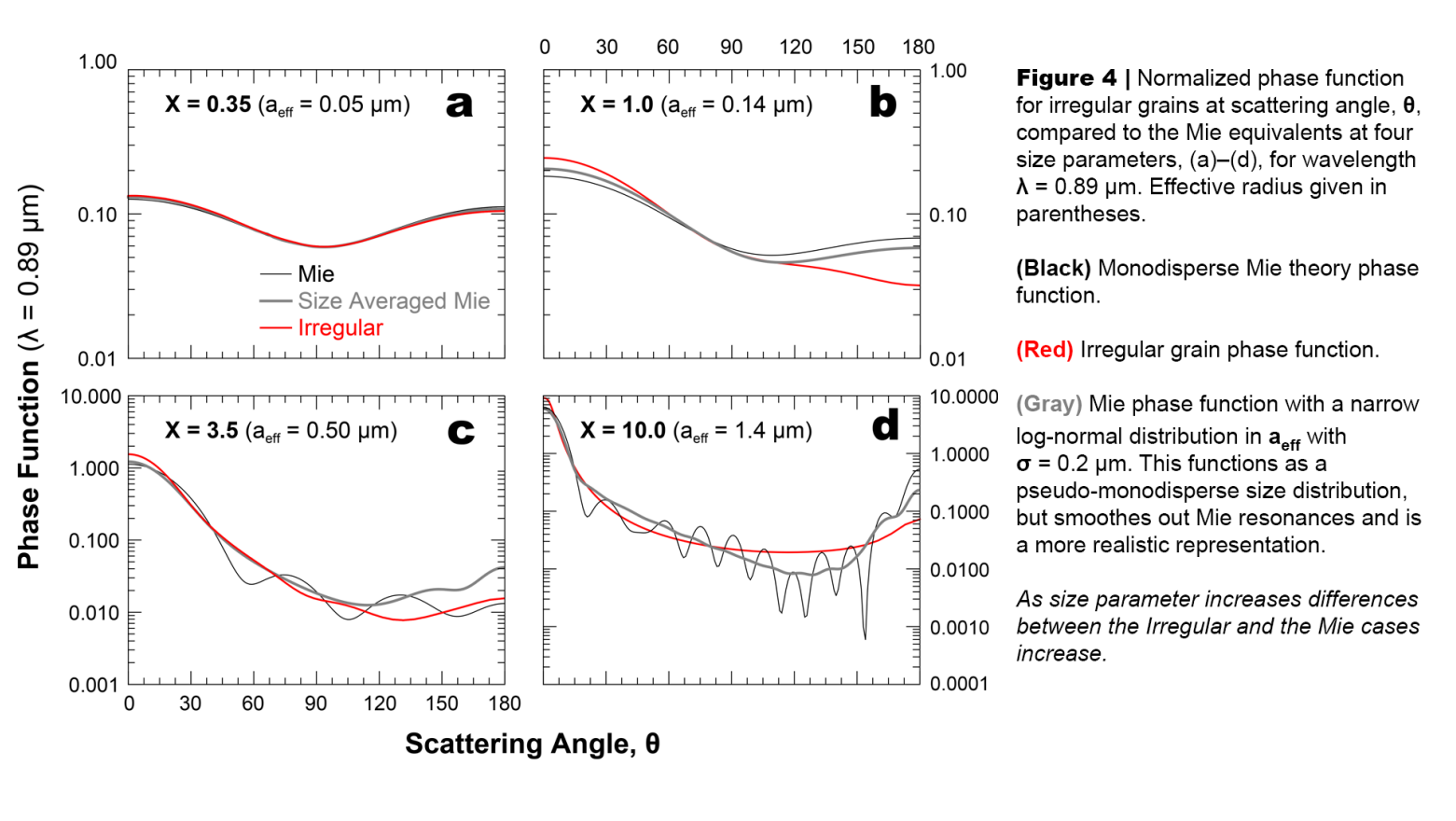

Figure 4 | *Normalized phase function for irregular grains at scattering angle,* **θ**, *compared to the Mie equivalents at four size parameters, (a)–(d), for wavelength* **λ** *= 0.89 µm. Effective radius given in parentheses.* ***(Black)*** *Monodisperse Mie theory phase function.* ***(Red)*** *Irregular grain phase function.* ***(Gray)*** *Mie phase function with a narrow log-normal distribution in aeff with* **σ** *= 0.2 µm. This functions as a pseudo-monodisperse size distribution, but smoothes out Mie resonances and is a more realistic representation.* ***As size parameter increases differences between the Irregular and the Mie cases increase.***

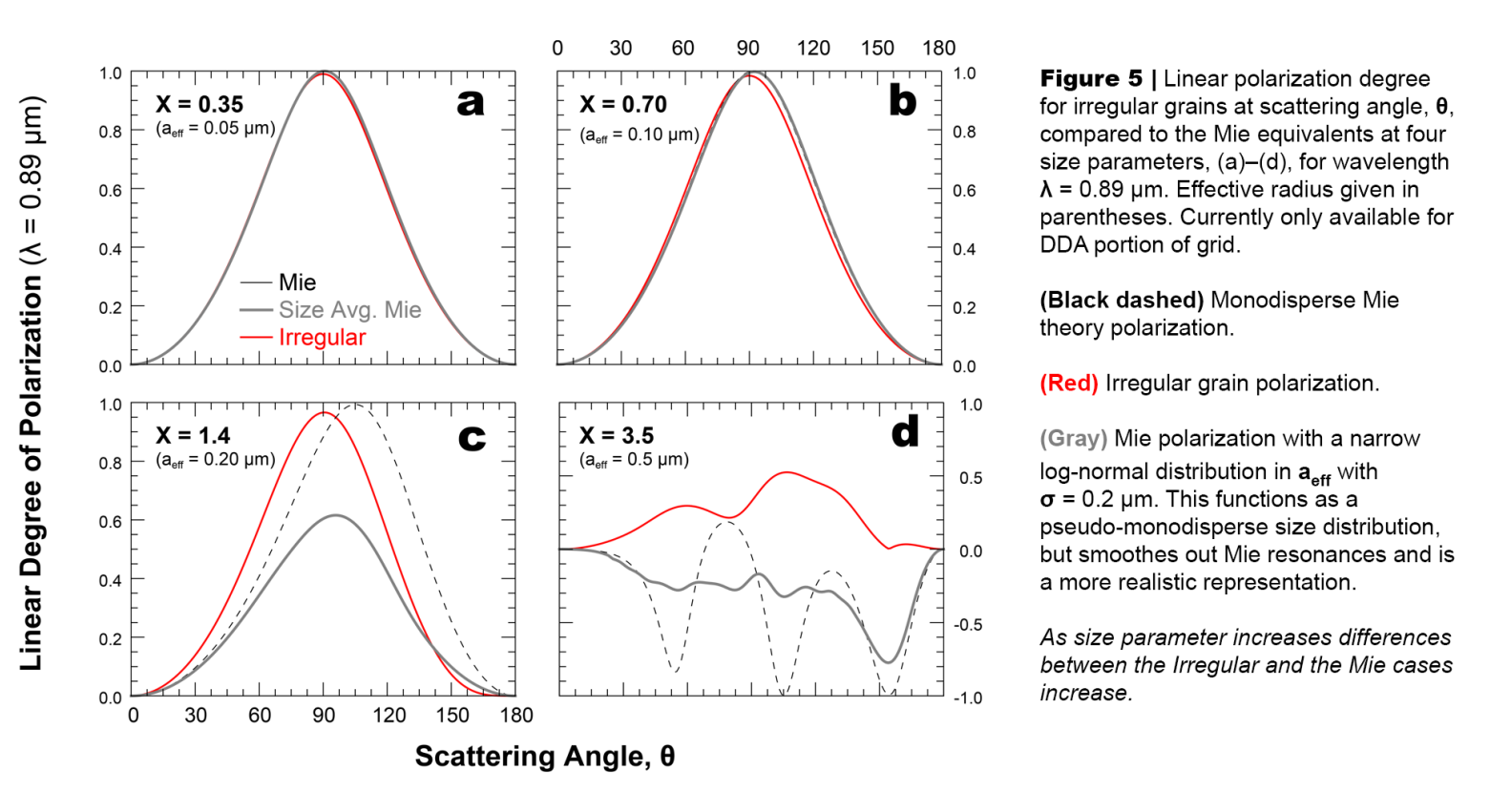

Figure 5 | *Linear polarization degree for irregular grains at scattering angle,* **θ**, *compared to the Mie equivalents at four size parameters, (a)–(d), for wavelength* **λ** *= 0.89 µm. Effective radius given in parentheses. Currently only available for DDA portion of grid.* ***(Black)*** *Monodisperse Mie theory polarization.* ***(Red)*** *Irregular grain polarization.* ***(Gray)*** *Mie polarization with a narrow log-normal distribution in* **a$_{eff}$** *with* **σ** *= 0.2 µm. This functions as a pseudo-monodisperse size distribution, but smoothes out Mie resonances and is a more realistic representation.* ***As size parameter increases differences between the Irregular and the Mie cases increase.***

Grid Validation

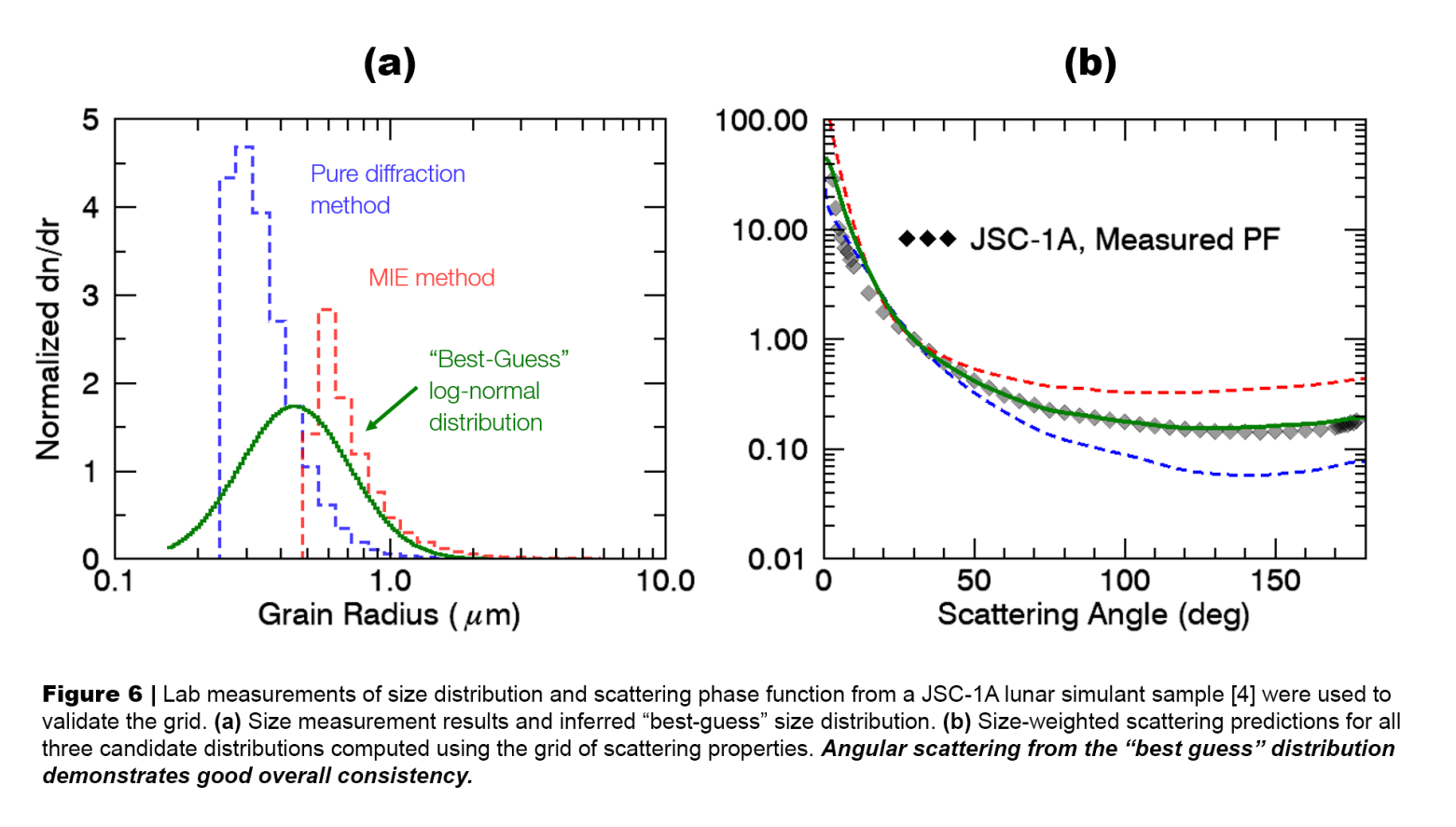

Figure 6 | *Lab measurements of size distribution and scattering phase function from a JSC-1A lunar simulant sample [4] were used to validate the grid.* ***(a)*** *Size measurement results and inferred "best-guess" size distribution.* ***(b)*** *Size-weighted scattering predictions for all three candidate distributions computed using the grid of scattering properties.* ***Angular scattering from the "best guess" distribution demonstrates good overall consistency.***

APPLICATIONS OF GRID

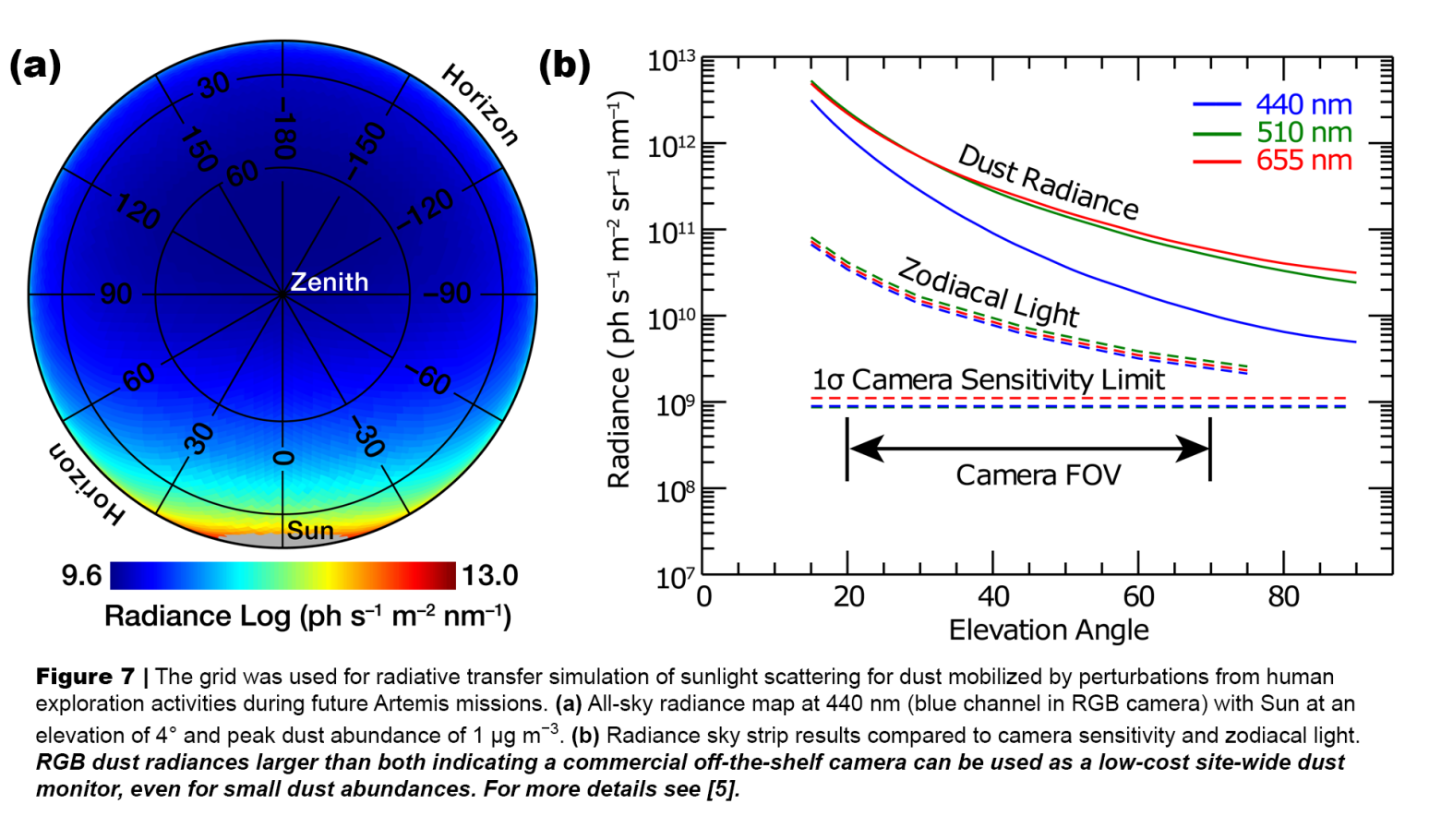

Figure 7 | *The grid was used for radiative transfer simulation of sunlight scattering for dust mobilized by perturbations from human exploration activities during future Artemis missions.* ***(a)*** *All-sky radiance map at 440 nm (blue channel in RGB camera) with Sun at an elevation of 4° and peak dust abundance of 1 µg m^{-3}.* ***(b)*** *Radiance sky strip results compared to camera sensitivity and zodiacal light.* ***RGB dust radiances larger than both indicating a commercial off-the-shelf camera can be used as a low-cost site-wide dust monitor, even for small dust abundances. For more details see [5].***

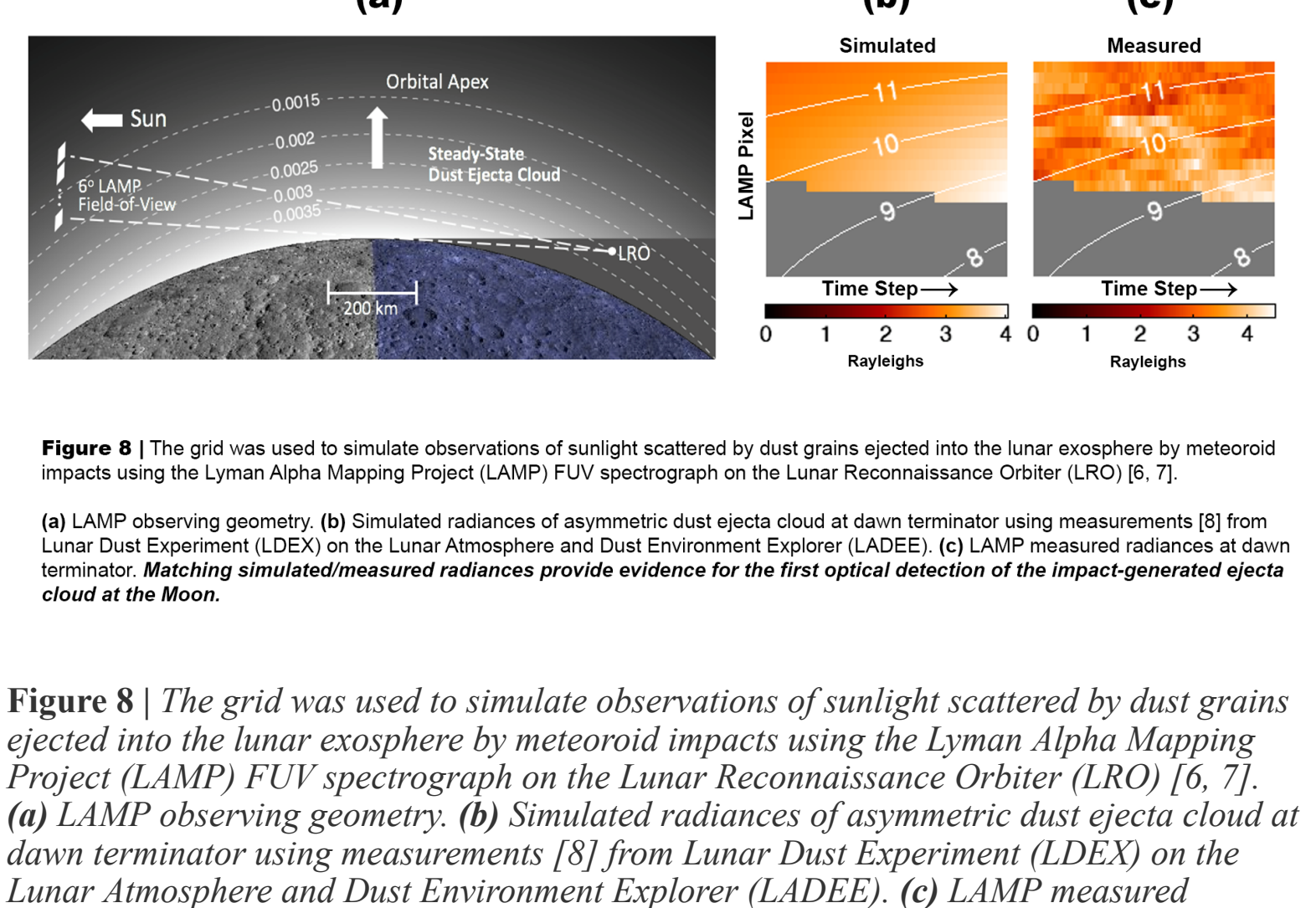

Figure 8 | *The grid was used to simulate observations of sunlight scattered by dust grains ejected into the lunar exosphere by meteoroid impacts using the Lyman Alpha Mapping Project (LAMP) FUV spectrograph on the Lunar Reconnaissance Orbiter (LRO) [6, 7].* ***(a)*** *LAMP observing geometry.* ***(b)*** *Simulated radiances of asymmetric dust ejecta cloud at dawn terminator using measurements [8] from Lunar Dust Experiment (LDEX) on the Lunar Atmosphere and Dust Environment Explorer (LADEE).* ***(c)*** *LAMP measured radiances at dawn terminator.* ***Matching simulated/measured radiances provide evidence for the first optical detection of the impact-generated ejecta cloud at the Moon.***

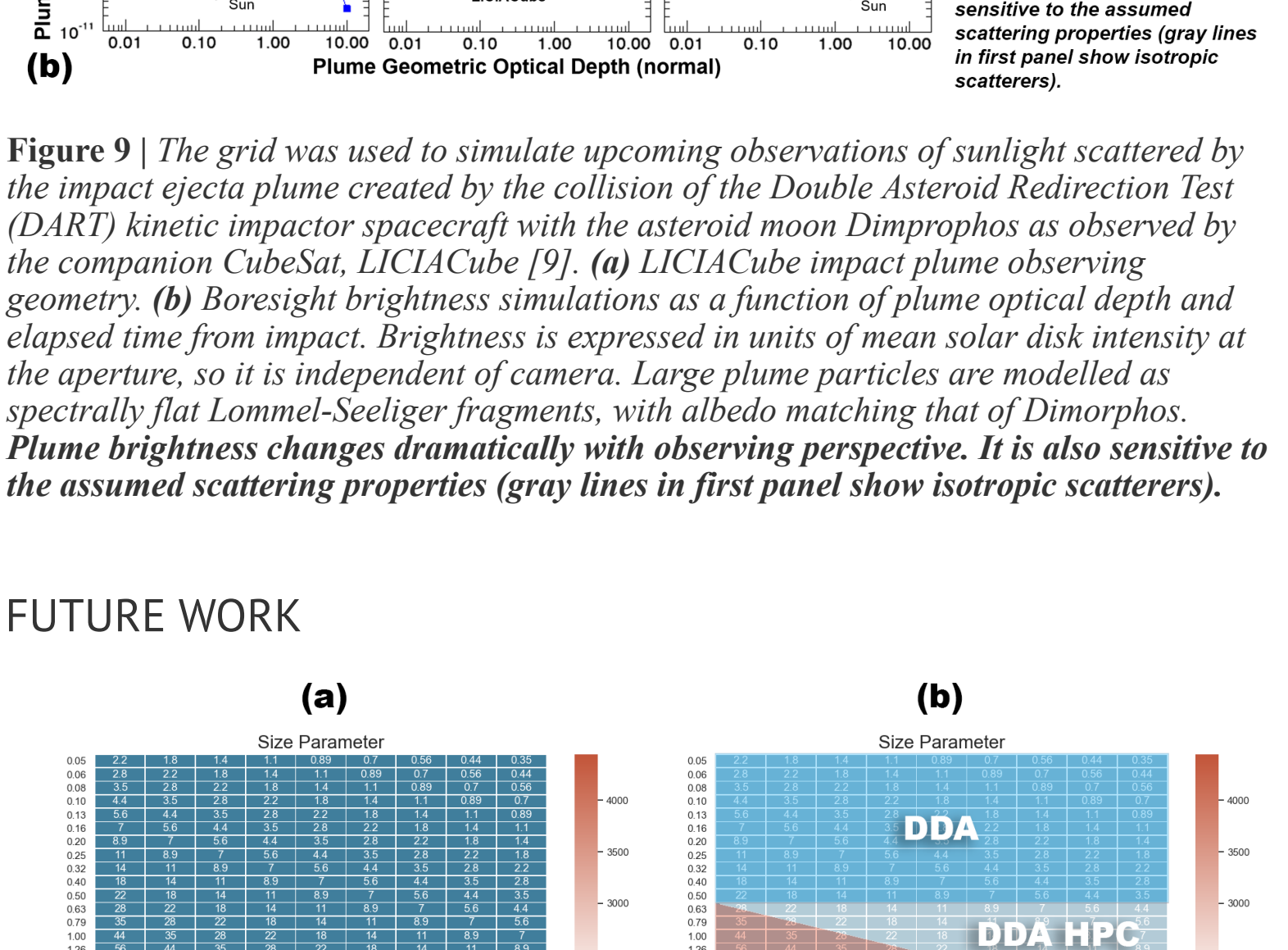

Figure 9 | *The grid was used to simulate upcoming observations of sunlight scattered by the impact ejecta plume created by the collision of the Double Asteroid Redirection Test (DART) kinetic impactor spacecraft with the asteroid moon Dimprophos as observed by the companion CubeSat, LICIACube [9].* ***(a)*** *LICIACube impact plume observing geometry.* ***(b)*** *Boresight brightness simulations as a function of plume optical depth and elapsed time from impact. Brightness is expressed in units of mean solar disk intensity at the aperture, so it is independent of camera. Large plume particles are modelled as spectrally flat Lommel-Seeliger fragments, with albedo matching that of Dimorphos.* ***Plume brightness changes dramatically with observing perspective. It is also sensitive to the assumed scattering properties (gray lines in first panel show isotropic scatterers).***

FUTURE WORK

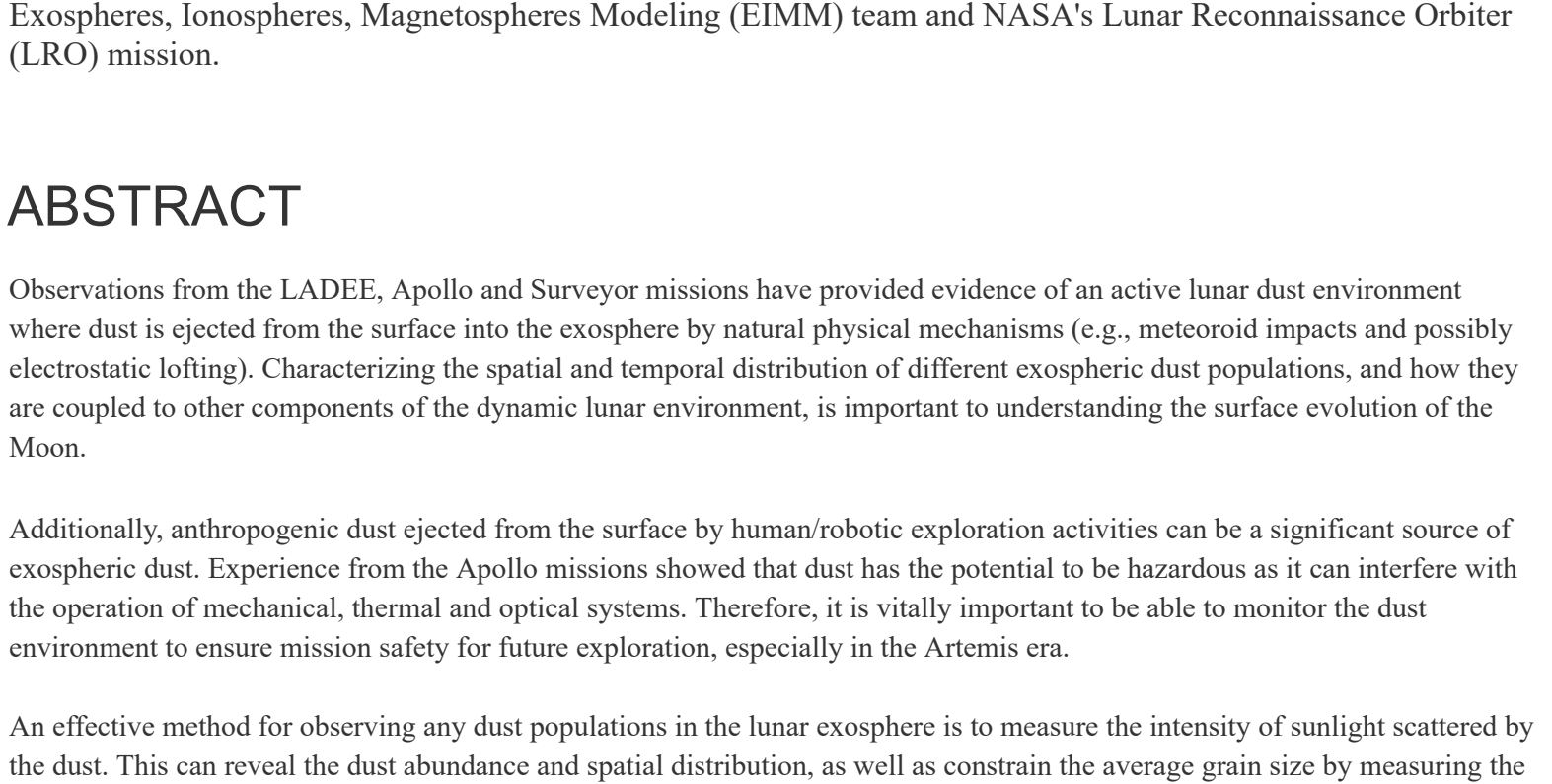

Figure 10 | ***(a)*** *Size parameter (**X = 2πa$_{eff}$/λ**) heat map of scattering grid.* ***(b)*** *Grid with overlays showing future expansion: Existing DDA coverage [2] (blue), DDA expansion region via High Performance Computing (white), and geometric optics with ray tracing (red).*

Future work (currently ongoing) to extend the capability of the grid:

- Expand DDA scope of grid to size parameter **X** = 22, this requires High Performance Computing. As **X** increases, using DDA becomes increasingly computationally expensive to model. Hence the need for another approach at larger grain sizes.
- Replace Hapke/Allen method with full geometric optics (using SIRIS software [10]) for grain sizes up to 100 µm for **X** > 22.
- These improvements will increase accuracy and make polarization available at all sizes.

Acknowledgments

This work has been funded by funded by the NASA/GSFC Internal Scientist Funding Model (ISFM) Exospheres, Ionospheres, Magnetospheres Modeling (EIMM) team and NASA's Lunar Reconnaissance Orbiter (LRO) mission.

ABSTRACT

Observations from the LADEE, Apollo and Surveyor missions have provided evidence of an active lunar dust environment where dust is ejected from the surface into the exosphere by natural physical mechanisms (e.g., meteoroid impacts and possibly electrostatic lofting). Characterizing the spatial and temporal distribution of different exospheric dust populations, and how they are coupled to other components of the dynamic lunar environment, is important to understanding the surface evolution of the Moon.

Additionally, anthropogenic dust ejected from the surface by human/robotic exploration activities can be a significant source of exospheric dust. Experience from the Apollo missions showed that dust has the potential to be hazardous as it can interfere with the operation of mechanical, thermal and optical systems. Therefore, it is vitally important to be able to monitor the dust environment to ensure mission safety for future exploration, especially in the Artemis era.

An effective method for observing any dust populations in the lunar exosphere is to measure the intensity of sunlight scattered by the dust. This can reveal the dust abundance and spatial distribution, as well as constrain the average grain size by measuring the angular width of the forward scattering lobe.

The largest uncertainties in such measurements lies in the grain scattering properties, namely: scattering coefficient, phase function shape and polarization. All of these become more important at larger scattering angles, where diffraction no longer dominates. Typically, the dust size distribution cannot be measured uniquely, and must be constrained by a set of forward simulations at multiple wavelengths and scattering angles.

We present a precomputed grid of light scattering properties for irregularly shaped grains (Richard et al., 2011), which are a more realistic representation of lunar dust than the Mie models commonly employed. The grid spans UV to near-IR wavelengths and encompasses a wide range of grain size. Scattering from smaller grains is computed using the Discrete Dipole (DDA) method (DDSCAT) and at larger sizes using the Hapke-Equivalent Slab with Allen diffraction (this will soon be replaced by ray tracing with diffraction). Applications of this grid include observation interpretation and modelling of sunlight scattered by meteoroid impact plumes, lunar horizon glow, and exploration activities.

REFERENCES

[1] *Wagner, S. 2012*, The Apollo experience lessons learned for Constellation lunar dust management (PDF). TP-2006-21 3726. Johnson Space Center, Houston.

[2] *Richard, D. et al. 2011*. Light scattering by complex particles in the Moon's exosphere, Planetary and Space Science, 59, 1804–1814.

[3] *Shkuratov, Y. et al. 1999*. A Model of Spectral Albedo of Particulate Surfaces: Implications for Optical Properties of the Moon, Icarus, Volume 1 37, Issue 2, 235–246.

[4] *Escobar-Cerezo et al. 2018*. An Experimental Scattering Matrix for Lunar Regolith Simulant JSC-1 A at Visible Wavelengths, The Astrophysical Journal Supplement Series, Volume 235, Issue 1, article id. 19, 9.

[5] *Lolachi R., et al. 2020.* Optical monitoring of the dust environment at lunar surface exploration sites, NASA Exploration Science Forum 2020, NESF2020-013, https://lunarscience.arc.nasa.gov/nesf2020/poster/optical-monitoring-of-the-dust-environment-at-lunar-surface-exploration-sites.

[6] *Glenar, D. A. et al. 2020.* Detection of the Impact-Generated Lunar Ejecta Cloud by LRO/LAMP, The Impact of Lunar Dust on Human Exploration, held 11–13 February, 2020 in Houston, Texas. LPI Contribution No. 2141, 2020, id.5033.

[7] *Stubbs, T. J. et al. 2019.* Evidence for the First Optical Detection of the Impact-generated Ejecta Cloud at the Moon, American Geophysical Union, Fall Meeting 2019, abstract #P21B-06.

[8] *Horányi, M. et al. 2015.* A permanent, asymmetric dust cloud around the Moon. Nature 522, 324–326.

[9] *Cheng, A. F. et al. 2020.* DART mission determination of momentum transfer: Model of ejecta plume observations. Icarus, 352, 113989.

[10] *Muinonen, K. et al. 2009.* Light scattering by Gaussian particles with internal inclusions and roughened surfaces using ray optics. Journal of Quantitative Spectroscopy and Radiative Transfer, 110, 1628–1639.